Operation of a TES microcalorimeter cooled by a compact liquid-helium-free ^3He-^4He dilution refrigerator directly coupled to a Gifford-McMahon cooler

Umeno, Takahiro
Department of Applied Quantum Physics and Nuclear Engineering, Kyushu University | Taiyo Nippon Sanso Corporation

Maehata, Keisuke
Department of Applied Quantum Physics and Nuclear Engineering, Kyushu University

Ishibashi, Kenji
Department of Applied Quantum Physics and Nuclear Engineering, Kyushu University

Kamioka, Yasuharu
Taiyo Nippon Sanso Corporation

他

出版情報：Cryogenics. 50 (5), pp.314-319, 2010-05-01. Elsevier
バージョン：

Operation of a TES Microcalorimeter Cooled by a Compact Liquid-Helium-Free ^3He-^4He Dilution Refrigerator Directly Coupled to a Gifford-McMahon Cooler

T. Umeno[a, b], K. Maehata[a*], K. Ishibashi[a], Y. Kamioka[b], S. Yoshida[b], K. Takasaki[c] and K. Tanaka[d]

[a]Department of Applied Quantum Physics and Nuclear Engineering, Kyushu University, Fukuoka-shi, 819-0395, Japan

[b]Taiyo Nippon Sanso Corporation, 1-3-26 Koyama, Shinagawa-ku, 142-8558, Japan

[c]Japan Atomic Energy Agency, 4-33 Muramatsu, Tokai-mura, Naka-gun, Ibaraki-ken, 319-1194, Japan

[d]SII NanoTechnology Inc., 36-1 Takenoshita, Oyama-cho, Suntou-gun, Shizuoka-ken, 410-1393, Japan

Abstract: A superconducting transition edge thermosensor (TES) microcalorimeter was irradiated with LX-ray photons emitted by an ^{241}Am source maintained at an operating temperature of 120 mK using a compact liquid-helium-free ^3He-^4He dilution refrigerator directly coupled to a Gifford-McMahon (GM) cooler. The first and second stages of the GM cooler were directly coupled to the first and second pre-cool heat exchangers of a stick shaped dilution unit through copper plates in a vacuum chamber. The helium-free dilution refrigerator provided a cooling power of 20 μW at 100 mK. Detection signals of LX-ray photons emitted by the ^{241}Am source were observed by operating the TES microcalorimeter in a severe noise environment induced by the mechanical vibrations of the GM cooler.

Keywords: Microcalorimeters (D), Dilution (E), Gifford-McMahon (E)

*Corresponding Author:
K. Maehata, Department of Applied Quantum Physics and Nuclear Engineering, Kyushu University, Fukuoka-shi, 819-0395, Japan
TEL: +81-92-802-3481 FAX: +81-92-802-3481
E-mai: maehata@nucl.kyushu-u.ac.jp

1. Introduction

Plutonium isotopes are handled with special care in nuclear fuel cycle plants such as reprocessing plants, mixed oxide fuel fabrication plants and so on. It is important to monitor transuranium elements quantitatively with high sensitivity and reliability for protection against leakage of plutonium isotopes. Although mono energy α particles are emitted by most transuranium elements during nuclear decay, the short range of α particles in matter causes difficulty in monitoring transuranium elements by counting the α particles. Most transuranium elements radiate γ- and/ or X-rays following their α decay. In the α decay of the ^{239}Pu isotope typical values of the emission probability of LX-ray with 11.6–20.7 keV, K_{α}X-ray with 94.7-98.4 keV, K_{β}X-ray with 110-115 keV, and γ-ray with 38.7-129 keV are 4.66 %, 0.0108 %, 0.0182 % and 0.0331 %, respectively [1]. When comparing the values of emission probability, LX-ray is used to monitor the plutonium isotopes using the photon counting technique.

For the radiation protection of workers in nuclear fuel cycle plants, it is necessary to estimate the internal exposure dose with high precision by monitoring the level of intake of plutonium isotopes. In vivo counting of LX-ray photons is employed to do this. The emission probability of LX-ray photons in the α-decay of plutonium isotopes is one of the most important parameters for high precision estimation of the level of intake of plutonium isotopes using this method. The value of the emission probability is estimated by analyzing an experimental energy spectrum of LX-ray photons emitted by the plutonium isotopes. LX-ray spectroscopy with insufficient energy resolution causes difficulty in determining the values of the emission probability. The width of the full energy peaks of LX-ray photons in the energy spectrum needs to be narrow for precise estimation. It is necessary to obtain the value of the full width at half the maximum (FWHM) below 100 eV for full energy peaks in the experimental energy spectrum.

A superconducting transition edge sensor (TES) microcalorimeter has the potential for precise analysis of transuranium elements by energy dispersive measurement of LX-ray photons in nuclear fuel cycle plants such as reprocessing plants, mixed oxide fuel fabrication plants and so on. A typical TES microcalorimeter is operated at cryogenic temperatures below the phase transition temperature of 200 mK for detecting X-ray photons. Usually, a ^{3}He-^{4}He dilution refrigerator is used to maintain the TES microcalorimeter at the operating temperature. Although liquid helium is consumed as a coolant in the operation of typical dilution refrigerators, it is difficult to use liquid helium in most laboratories that handle nuclear fuel and transuranium elements. Furthermore, a compact structure is needed to operate the TES microcalorimeter for the detection of LX-ray photons emitted by transuranium elements in nuclear plants.

Recently, a liquid-helium-free dilution refrigerator has been developed by using a Gifford-McMahon (GM) cooler for pre-cooling the gaseous ^{3}He-^{4}He mixture [2]. The reciprocal motion of the displacer of the GM cooler induces mechanical vibrations in the dilution components. However, degradation in the operational performance has not yet been studied for the TES microcalorimeter subjected to the mechanical vibration induced by the GM cooler.

In this work, a compact liquid-helium-free ^{3}He-^{4}He dilution refrigerator pre-cooled by the GM cooler was developed for exploring the feasibility of the TES microcalorimeter operation. A TES microcalorimeter was irradiated with LX-ray photons emitted by a ^{241}Am source while maintaining an operating temperature of 120 mK by using the compact liquid-helium-free ^{3}He-^{4}He dilution refrigerator.

2. TES microcalorimeter

The TES microcalorimeter is a thermal detector that measures the energy of an incident photon as the temperature rises [3]. Fig. 1 shows an operating configuration for the TES microcalorimeter. The TES microcalorimeter consists of a superconducting thin film thermometer and an energy absorber. The superconducting thin film thermometer of the TES microcalorimeter exhibits a sharp transition edge between superconducting and normal conducting states as shown in the inset of an $R\!-\!T$ curve in Fig. 1. The TES chip is thermally connected to a cold bath at temperature T_b through a conducting heat link G. In the TES electrical circuit, a coil L is connected in series with the TES, and a shunt resistor R_S is connected in parallel with the TES$-L$ line. A constant dc bias current I_{Bias} supplied to the TES electrical circuit is divided into the TES current I_{TES} and the shunt current I_S as shown Fig. 1. The energy of incident X-ray photons is converted into the temperature rise ΔT in the absorber. The temperature rise ΔT induces a steep growth in the electrical resistance of the TES by ΔR. The resistance growth ΔR causes a reduction of ΔI_{TES} in the TES current I_{TES}. The coil L generates the change in the magnetic flux $\Delta\varphi$ across a superconducting quantum interference device (SQUID). As shown in the inset in Fig. 1, the magnetic flux change $\Delta\varphi$ is converted into a voltage signal pulse by the SQUID amplifier.

SII NanoTechnology Inc has developed a TES microcalorimeter, exhibiting excellent energy resolution for an X-ray energy dispersive spectrometer (EDS) that can be installed in a scanning electron microscope (SEM) [4]. The TES microcalorimeter consists of a thin film thermometer that has a bilayer structure of Au/Ti with the absorber Au layer deposited on the thermometer film. The Au absorber, 0.5μm thick, allows the TES microcalorimeter to detect X-ray photons with energies of 300 eV to 6 keV emitted by a sample in the SEM, with an absorption efficiency above 50 %. Since the energy of LX rays emitted by transuranium elements ranges from 10 to 20 keV, the TES microcalorimeter for the SEM-EDS has insufficient absorption efficiency for the LX-ray detection.

In this work, the TES microcalorimeter of X-ray fluorescence analysis was modified to detect LX-ray photons emitted by transuranium elements. The thickness of the Au absorber was set to be 5.0 μm for an absorption efficiency of 50 % and a counting rate of 100 counts per second for the detection of LX-ray photons with energy from 10 to 20 keV. For the convenience of refrigerator operation, the phase transition temperature of the TES was designed to be 200 mK by using the proximity effect between Au and Ti at 120 and 50 nm thick, respectively. The geometrical dimensions of the thermometer and the absorber are 300 x 300 μm^2 and 500 x 500 μm^2. The designed TES chip was fabricated by SII NanoTechnology Inc. The fabricated TES microcalorimeter was demonstrated to detect LX-ray of 17.75 keV emitted by ^{237}Np after the α decay of the ^{241}Am isotope in experiments, using a dilution refrigerator pre-cooled by liquid helium [5].

3. Compact liquid-helium-free ^3He-^4He dilution refrigerator

A compact liquid-helium-free ^3He-^4He dilution refrigerator pre-cooled by the GM cooler was developed for exploring the feasibility of the TES microcalorimeter operation. Fig. 2 shows a schematic diagram of the compact liquid-helium-free ^3He-^4He dilution refrigerator. The dilution components of the heat exchangers, the still and the mixing chamber are assembled into a stick shaped compact structure with a maximum outer diameter of 24 mm and is 1000 mm long. The stick shaped dilution unit is inserted into a sheath attached to the top flange of the vacuum chamber. At the top of the sheath, the Wilson-seal structure provides the leak-tight condition of the dilution unit. The gaseous ^3He-^4He mixture is circulated by the rotary vane pump (Alcatel 2033H1). The circulating gaseous ^3He-^4He mixture is pre-cooled by operating the GM cooler (Sumitomo Heavy Industry RDK-408D) with 2 stages placed on the top flange of the vacuum chamber. The values of the cooling power of the first and second stages are 37 W at 40 K, and 1 W at 4.2 K. For pre-cooling the warm gaseous ^3He-^4He mixture, the first and second stages of the GM cooler are directly coupled to the heat exchangers HX1 and HX2 of the stick shaped dilution unit, through copper plates in the vacuum chamber.

After sufficient pre-cooling through the heat exchanger HX3, the gaseous ^3He-^4He mixture is condensed by the isoenthalpic expansion through the impedance Z1 and flows into the concentrated

^{3}He mixture. The concentrated ^{3}He mixture flows through the heat exchanger HX4 and enters the heat exchanger HX5. In the HX5, the concentrated ^{3}He mixture flows in the capillary coiled around a plunger cooled by the diluted ^{3}He mixture flowing in the channel between the inner surface of the sheath and outer surface of the coiled capillary. After cooling in the HX5, the concentrated ^{3}He mixture enters the mixing chamber 1 (MC1) of a cascade of two mixing chambers. A part of the flow of the concentrated ^{3}He mixture is diluted in MC1 and returns to the dilute flow channel in the heat exchanger through the flow impedance Z2. The other part of the concentrated ^{3}He mixture is pre-cooled to the temperature of the mixing chamber 2 (MC2) through the heat exchanger HX6, which has a similar structure to the HX5. The concentrated ^{3}He mixture entering the MC2 is diluted and returns to the still through HX6 and HX5. The concentrated ^{3}He mixture gas is pumped out of the still and flows toward the circulation pump through the heat exchangers. Experimental samples are placed on the holder plate attached to the base plate of MC2.

The liquid-helium-free ^{3}He-^{4}He dilution refrigerator was operated without sampling for a cool-down test. Fig. 3 shows a trend of temperatures indicated by the thermometers mounted on the MC1, MC2, Still and HX2 as shown in Fig.2. After the GM cooler had operated for 24 hours, the heat exchanger HX2 was cooled to a temperature of 4.0 K from 3000K and the gaseous ^{3}He-^{4}He mixture started to circulate. It took 60 minutes to take the temperature of the MC2 below 100 mK while circulating the gaseous ^{3}He-^{4}He mixture. The inlet pressure of the circulating ^{3}He mixture gas was stabilized at 0.102 MPa. The temperature of the MC2 dropped to 50 mK with the still temperature at 1.05 K. Fig. 4 shows the temperature dependence of the cooling power of the liquid-helium-free ^{3}He-^{4}He dilution refrigerator. The cooling power achieved by the MC2 was 20 μW at 100 mK.

4. Detection of LX-ray photons emitted by ^{241}Am source

The fabricated TES microcalorimeter chip was mounted on the TES holder of the liquid-helium-free ^{3}He-^{4}He dilution refrigerator for the measurement of the electrical resistance and temperature (*R*-*T*) characteristics. The reciprocating motion of the displacer of the GM cooler induced mechanical vibrations in the TES holder during the operation of the dilution refrigerator. A lock-in amplifier using the four-wire method was employed for measuring electrical resistance. The lock-in frequency was taken to be 77 Hz to minimize the severe noise contribution. The values of the bias current were set to 1, 5 and 10 μA for suppressing the thermal disturbance caused by the Joule heat generation. The temperature of the TES microcalorimeter chip was controlled using a PID controller in the temperature range of 160 to 200 mK with a 5 mK step. Fig. 5 shows the resultant *R*-*T* characteristics. Although a steep growth of electrical resistance does not appear in Fig. 5 because of the wide step in the temperature increment, the phase transition region is found in the temperature region of 170 to 185 mK. The TES microcalorimeter chip was found to have an electrical resistance of 50 mΩ in the normal conducting state.

The SQUID amplifier chip was placed on the TES holder adjacent to the TES chip to reduce the noise voltage generated in the wirings connected to the SQUID input. The SQUID amplifier chip was fabricated by SII NanoTechnology Inc. Fig. 6 shows a circuit diagram of the TES microcalorimeter and the SQUID amplifier. A constant bias current was supplied to the TES-SQUID circuit from a precise current source outside the refrigerator, while the TES microcalorimeter was biased with a constant voltage generated by a shunt resistance of 7 mΩ. The reciprocating motion of the displacer of the GM cooler caused large periodic voltage pulses at the output of the SQUID amplifier. The voltage output of the SQUID amplifier was analyzed using a fast Fourier transform (FFT) for surveying noise components induced by the mechanical vibrations. Fig. 7(a) and Fig. 7(b) show the analyzed results of the noise spectrum with and without the GM cooler running, respectively. In Fig. 7(a), components of 1.2 Hz and higher harmonics indicate that the reciprocating motion of the displacer and the compact structure is caused by a mechanical vibration.

An ^{241}Am source with an intensity of 3.7 MBq was placed in front of the TES microcalorimeter. The surface of the ^{241}Am source was covered with a polyimide tape with sufficient thickness to stop α particles. When the TES microcalorimeter was operated by supplying the bias current of 600 μA at the mixing chamber temperature of 120 mK, voltage signal pulses of the SQUID amplifier were observed from the detection of LX-ray photons emitted by ^{237}Np after the α decay of the ^{241}Am. The rise and decay time constants of the signal pulses are 3 and 160 μs. The decay time constant of 160 μs implies an electrothermal-feedback operation mode and allows the TES microcalorimeter to operate with a counting rate higher than 100 counts per second. Figure 8 shows the pulse height distribution of the voltage signal pulses processed through a low-pass filter with a cut-off frequency of 50 kHz. The vertical axis indicates the number of counts of pulse heights within the bin-width of 1 mV. Peaks in Fig. 8 are labeled with the corresponding LX-ray photons by referring to the LX-ray energy emitted by the ^{237}Np after the α decay of the ^{241}Am. The signal current generated by the TES microcalorimeter was evaluated to be 2.5 μA / 10 keV by using the conversion gain of the SQUID amplifier. The energy resolution was evaluated to be 400 eV of full width at half the maximum level by analyzing the acquired pulse height distribution. A poor energy resolution may be caused by insufficient reduction of the various noise contributions in the liquid-helium-free ^{3}He-^{4}He dilution refrigerator. However, the

TES microcalorimeter with the 5.0 μm thick absorber was shown to detect the LX-ray photons emitted by the ^{241}Am source.

5. Conclusions

The TES microcalorimeter with an Au absorber 5.0 μm thick for the detection of LX-ray photons emitted by transuranium elements was cooled by operating the liquid-helium-free ^{3}He-^{4}He dilution refrigerator pre-cooled by the GM cooler. The TES and SQUID chips suffered from mechanical vibrations induced by the reciprocating motion of the displacer of the GM cooler. Detection signals of LX-ray photons emitted by the ^{241}Am source were observed by operating the TES microcalorimeter in the severe noise environment induced by mechanical vibrations. The decay time constant of the detection signal pulses allows the TES microcalorimeter to operate with a counting rate higher than 100 counts per second. Although the severe noise environment caused poor energy resolution of the 400 eV FWHM, the energy resolution is expected to improve by establishing the noise reduction technique.

Acknowledgment

This work is supported in part by a Grant-in-Aid for Scientific Research (A) (18206098) of the Japan Society for the Promotion of Science and the JAEA Cooperative Research Scheme on the Nuclear Fuel Cycle.

References

[1] BNM-LNHB/CEA Table de Radioneucléides, http://www.nucleide.org/DDEP_WG/DDEPdata.htm

[2] Uhlig K. Hehn W. $^{3}He/^{4}He$ dilution refrigerator pre-cooled by Gifford-McMahon refrigerator. Cryogenics 1997; 37: 279-82.

[3] Irwin K.D. An application of electrothermal feedback for high resolution cryogenic particle detection. Appl Phys Lett. 1995; 66: 1998-2000.

[4] Tanaka K. Odawara A. Nagata A. Ikeda M. Baba Y. Nakayama S. A microcalorimeter EDS system suitable for low acceleration voltage analysis. Surf Interface Anal. 2006; 38: 1646-9.

[5] Maehata K. Nakamura K. Yasumune T. Ishibashi K. Takasaki K., Tanaka K. Odawara A. Nagata A. Development of a TES Microcalorimeter for Spectroscopic Measurement of LX-rays Emitted by Transuranium Elements. submitted to J. Nucl. Sci. & Technol.

Figure Captions

Fig. 1 Operating configuration of the TES microcalorimeter

Fig. 2 Diagram of the compact liquid-helium-free ^{3}He-^{4}He dilution refrigerator

Fig. 3 Trend of temperatures indicated by the thermometers mounted on the mixing chambers and heat exchangers in the cool down test

Fig. 4 Temperature dependence of the cooling power

Fig. 5 R–T characteristics of the TES microcalorimeter with absorber thickness of 5.0μm

Fig. 6 Circuit diagram of the TES microcalorimeter and SQUID amplifier chips

Fig. 7(a) Noise spectrum of the voltage signals of the SQUID amplifier with the GM cooler running

Fig. 7(b) Noise spectrum of the voltage signals of the SQUID amplifier without the GM cooler running

Fig. 8 Pulse height distribution of detection signal pulses of LX-ray photons emitted by ^{237}Np following an α decay of the ^{241}Am

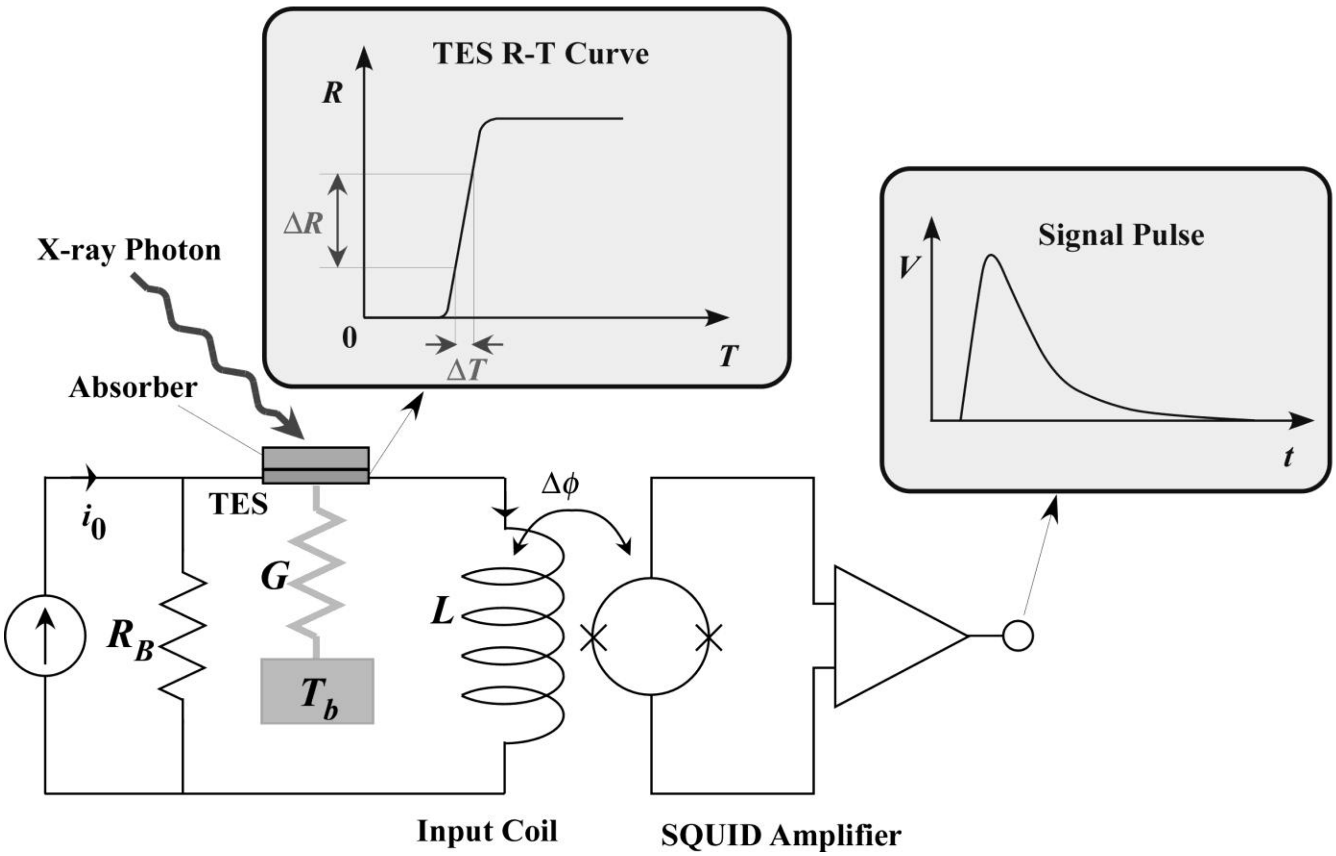

Fig. 1 Operating configuration of the TES microcalorimeter

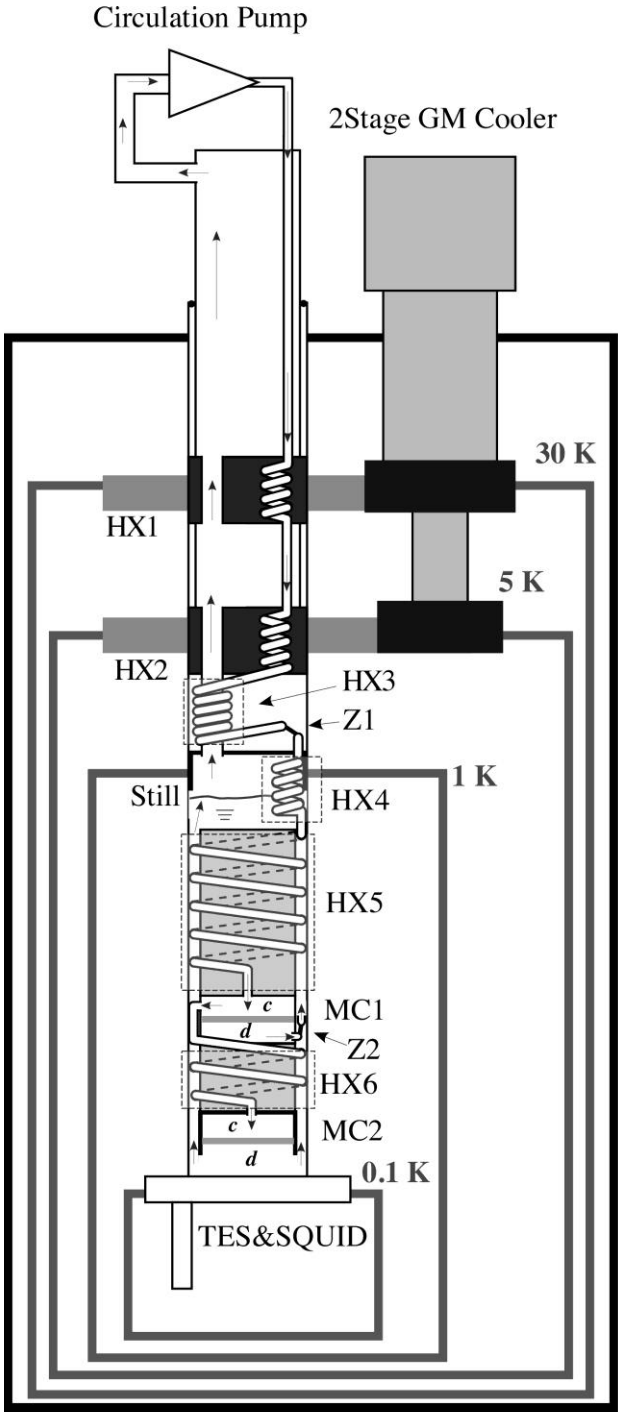

Fig. 2 Diagram of the compact liquid-helium-free ^3He-^4He dilution refrigerator

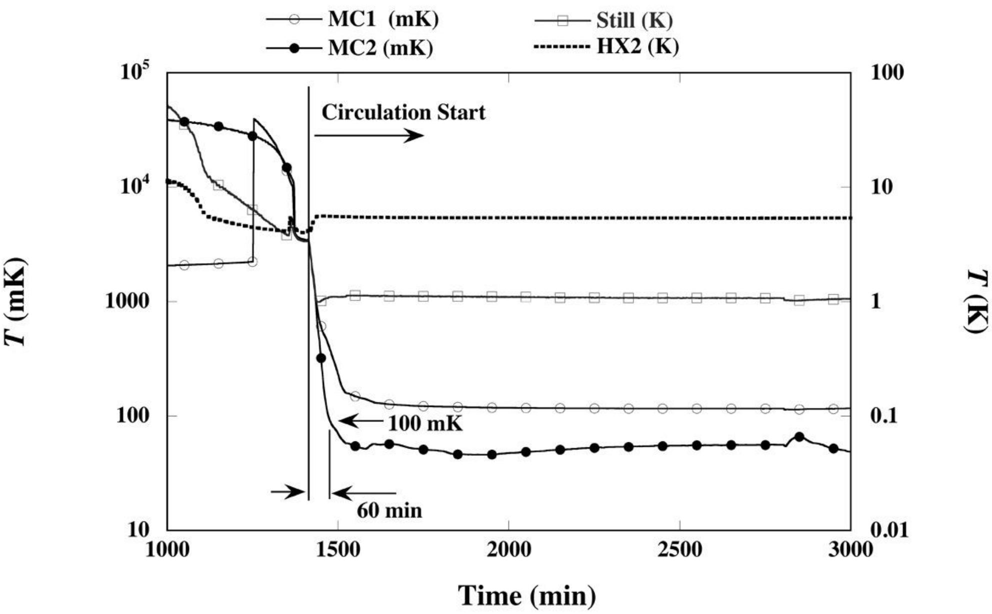

Fig. 3 Trend of temperatures indicated by the thermometers mounted on the mixing chambers and heat exchangers in the cool down test

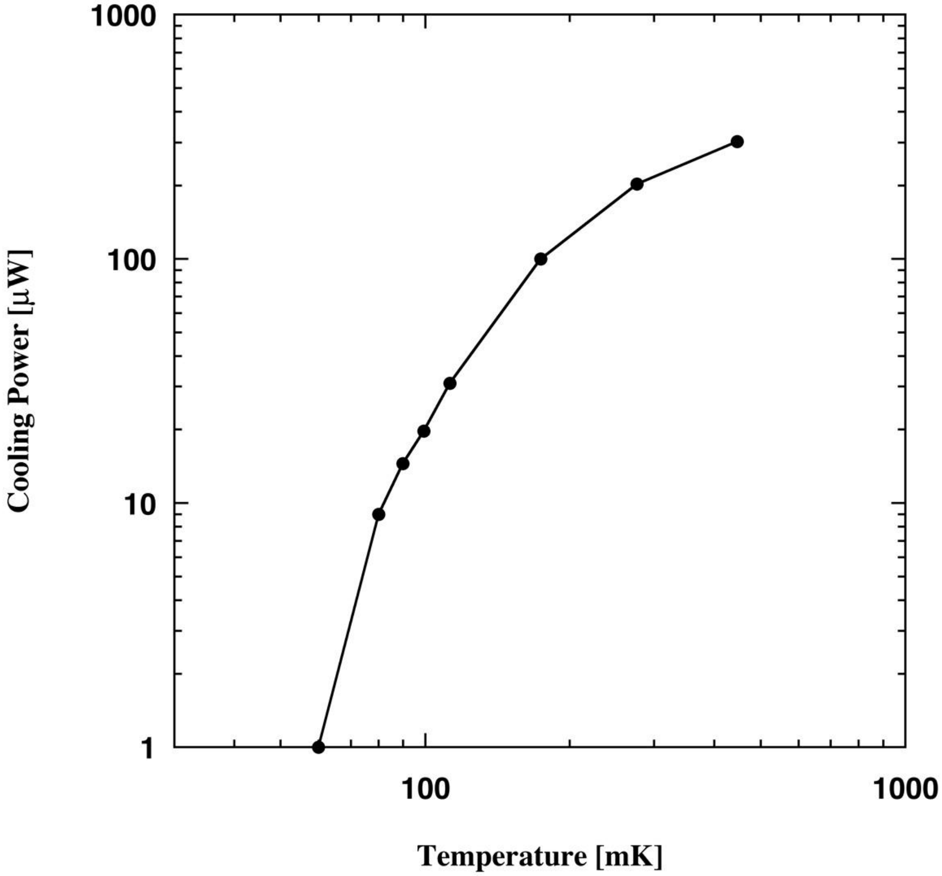

Fig. 4 Temperature dependence of the cooling power

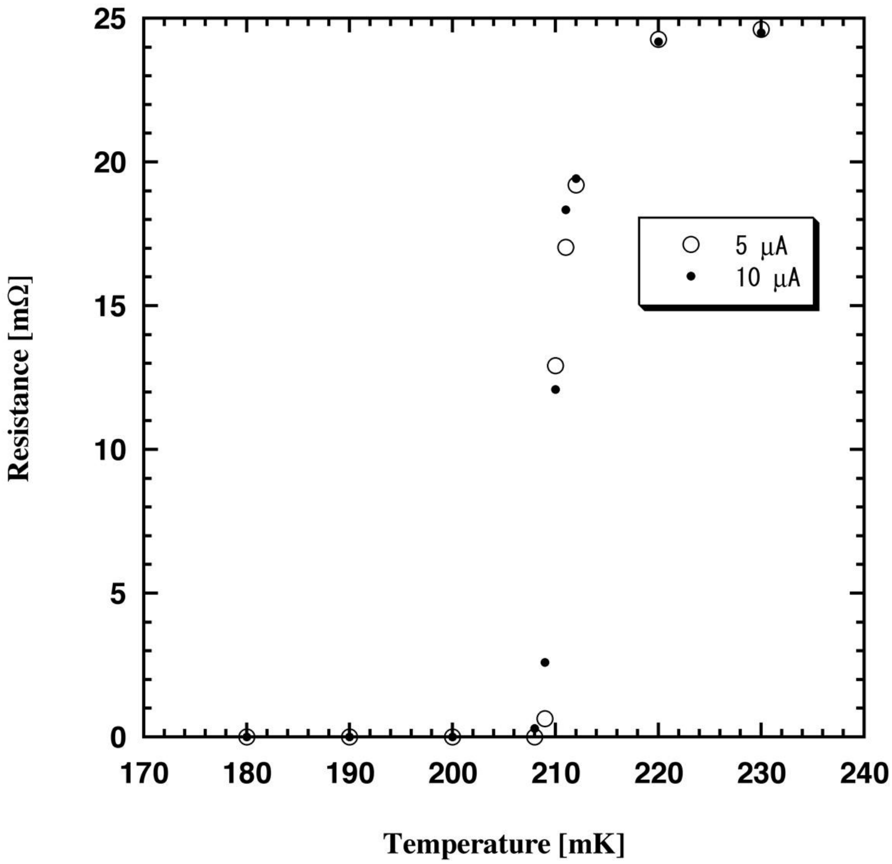

Fig. 5 *R–T* characteristics of the TES microcalorimeter with absorber thickness of 5.0μm

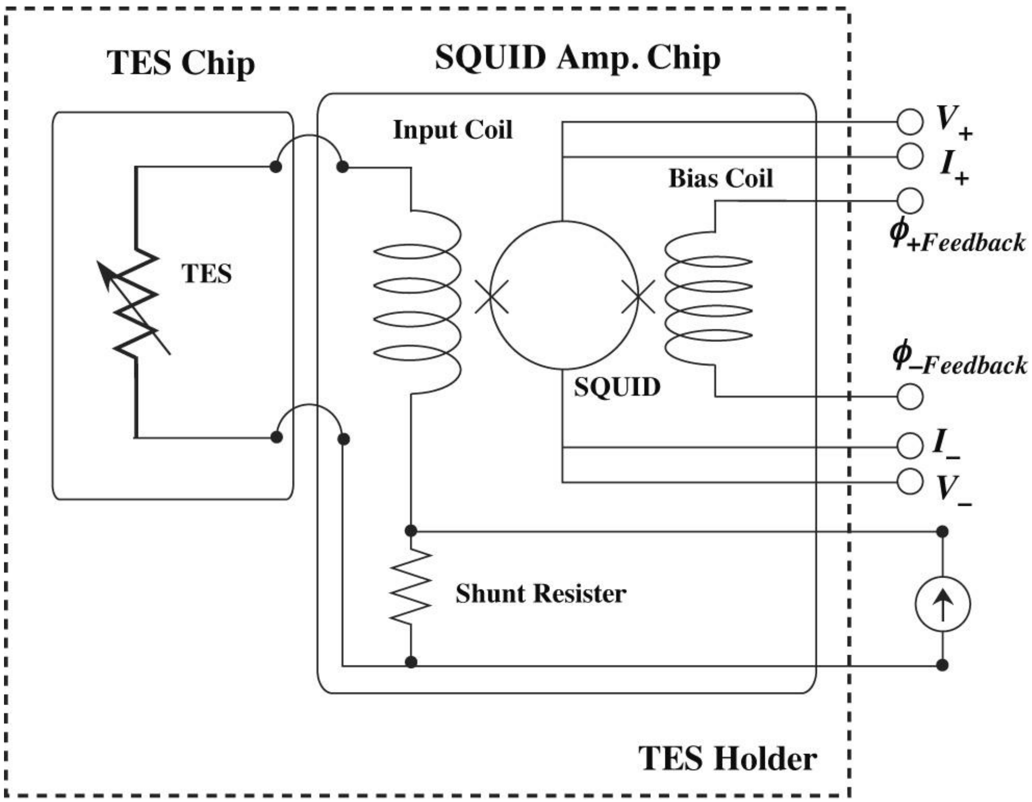

Fig. 6 Circuit diagram of the TES microcalorimeter and SQUID amplifier chips

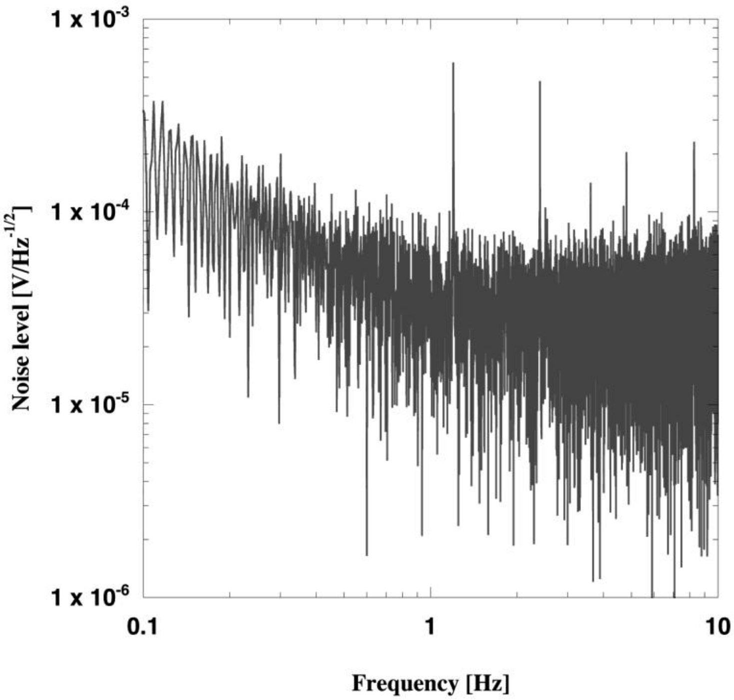

Fig. 7(a) Noise spectrum of the voltage signals of the SQUID amplifier with the GM cooler running

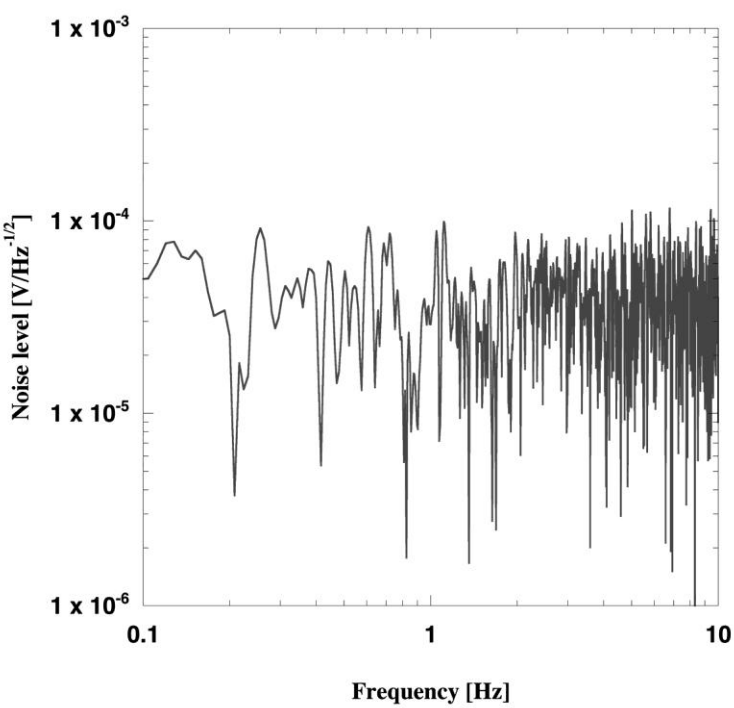

Fig. 7(b) Noise spectrum of the voltage signals of the SQUID amplifier without the GM cooler running

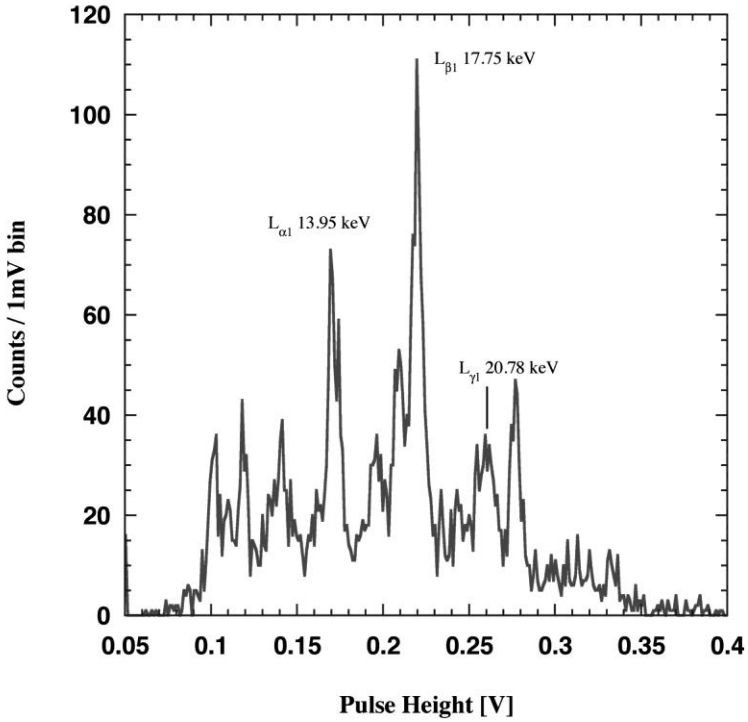

Fig. 8 Pulse height distribution of detection signal pulses of LX-ray photons emitted by ^{237}Np following an α decay of the ^{241}Am